HHS Public Access

Author manuscript

Mol Pharm. Author manuscript; available in PMC 2017 December 14.

Published in final edited form as:

Mol Pharm. 2016 June 06; 13(6): 2049–2058. doi:10.1021/acs.molpharmaceut.6b00187.

Combination Approach of YSA Peptide Anchored Docetaxel Stealth Liposomes with Oral Antifibrotic Agent for the Treatment of Lung Cancer

Ketan Patel[†], **Ravi Doddapaneni**[†], **Vasanthakumar Sekar**, **Nusrat Chowdhury**, and **Mandip Singh**[*]

College of Pharmacy and Pharmaceutical Sciences, Florida A&M University, Tallahassee, Florida 32307, United States

Abstract

Therapeutic efficacy of nanocarriers can be amplified by active targeting and overcoming the extracellular matrix associated barriers of tumors. The aim of the present study was to investigate the effect of oral antifibrotic agent (telmisartan) on tumor uptake and anticancer efficacy of EphA2 receptor targeted liposomes. Docetaxel loaded PEGylated liposomes (DPL) functionalized with nickel chelated phospholipid were prepared using a modified hydration method. DPL were incubated with various concentrations of histidine tagged EphA2 receptor specific peptide (YSA) to optimize particle size, zeta potential, and percentage YSA binding. Cellular uptake studies using various endocytosis blockers revealed that a caveolae dependent pathway was the major route for internalization of YSA anchored liposomes of docetaxel (YDPL) in A549 lung cancer cell line. Hydrodynamic diameter and zeta potential of optimized YDPL were 157.3 ± 11.8 nm and −3.64 mV, respectively. Orthotopic lung tumor xenograft (A549) bearing athymic nude mice treated with oral telmisartan (5 mg/kg) for 2 days showed significantly ($p < 0.05$) higher uptake of YDPL in tumor tissues compared to healthy tissue. Average lung tumor weight of the YDPL + telmisartan treated group was 4.8-and 3.8-fold lower than that of the DPL and YDPL treated groups ($p < 0.05$). Substantially lower expression ($p < 0.05$) of EphA2 receptor protein, proliferating cell nuclear antigen (PCNA), MMP-9, and collagen 1A level with increased E-cadherin and TIMP-1 levels in immunohistochemistry and Western blot analysis of lung tumor samples of the combination group confirmed antifibrotic effect with enhanced anticancer activity. Active targeting and ECM remodeling synergistically contributed to anticancer efficacy of YDPL in orthotopic lung cancer.

Graphical abstract

[*]**Corresponding Author**, Tel: (850) 561-2790. Fax: (850) 599-3813. mandip.sachdeva@famu.edu.

[†]**Author Contributions**

K.P. and R.D. have equally contributed to this paper.

ASSOCIATED CONTENT

Supporting Information

The Supporting Information is available free of charge on the ACS Publications website at DOI: 10.1021/acs.molpharmaceut.6b00187.

In vitro release study of various DTX formulations (PDF)

The authors declare no competing financial interest.

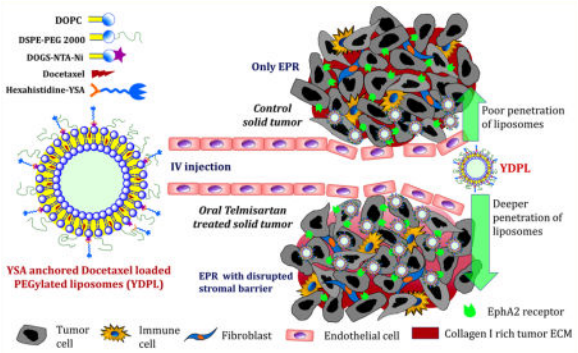

Keywords

EphA2 receptor; targeted drug delivery; docetaxel; extracellular matrix (ECM); orthotopic lung cancer; PEGylated liposomes

INTRODUCTION

Despite improved survival in certain subsets of lung cancer patients owing to novel therapeutic approaches, lung cancer is the leading cause of cancer related deaths worldwide.[1–3] Non-small cell lung cancer (NSCLC) is the most common type of lung cancer with overall 5-year survival rate <15%. Many of the small-molecular anticancer drugs have a large volume of distribution with narrow therapeutic window due to severe toxicities to normal tissues.[4] One major reason for poor therapeutic outcome of chemotherapy is compromised delivery of anticancer drug to the lung cancer tissues due to high tumor interstitial fluid pressures (TIFP). Leaky neovasculature, abnormal lymphatic drainage system, and perivascular fibrosis are associated with high interstitial fluid pressure.[5,6] Furthermore, lack of selectivity toward tumor tissue allows anticancer drugs to distribute indiscriminately between tumor and normal healthy tissues.[6,7] Consequently, cancer cells are exposed to relatively lower concentration of anticancer drug than normal cells, resulting in increased off target toxicities with reduced effectiveness. Therefore, it is very essential to develop therapeutic strategies to enhance the availability of drugs to tumor tissues while sparing healthy tissues.

Nanoparticulate systems have been extensively studied for passive and active targeted delivery of anticancer agents. Nanoparticles of <200 nm size are leaked from the tumor region and retained there, owing to abnormal tumor vasculature and lymphatic system driven enhanced permeability and retention effect (EPR).[8] Liposomal carriers have multiple advantages over other types of nanocarriers. Phospholipids are very safe and biocompatible excipients compared to nonionic surfactants and polymers for intravenous delivery.[9,10] Further, surface PEGylation to bypass the reticuloendothelial system, conjugation of targeted ligand, and large-scale manufacturing of liposomes can be accomplished by various technologies.[11] At present, most of the nanocarriers approved by the US Food and Drug Administration are liposomal carriers, e.g., Doxil, DepoCyt, Myocet, DaunoXome, Marqibo, etc.[7] Tumor targeted moieties are coupled to the surface of nanoliposomes to facilitate selective binding to tumor-specific antigens. Use of peptides as ligands to direct

nanoliposomes to tumors represents a potentially feasible approach to improve the clinical outcome. Anticancer drugs in the taxane class (paclitaxel and docetaxel) have severe solubility issues, which necessitates very large amount of ethanol and nonionic surfactant for their parenteral delivery.[12,13] There is no report describing physical stability of PEGylated liposomal docetaxel. Generally, the stability of nanocarrier developed for preclinical studies is sufficient to carry out in vitro experiments and animal studies, but for clinical application, long-term stability data is essential. Poor physical stability of docetaxel (DTX) loaded liposomes due to rapid precipitation of DTX is the major limiting factor for its clinical development. Therefore, an innovative method to formulate DTX loaded liposomes with extended stability is necessary.

Smoking remains the predominant cause of NSCLC with approximately 85% of NSCLC cases being associated with smokers.[14] EphA2 is found to be significantly associated in patients with smoking history and overexpressed in 90% of NSCLC tumors.[15,16] Cell membrane bound EphA2 receptor, a member of Eph tyrosine kinase receptor family, is composed of the EphA (EphA1–10) or EphB (EphB1–6) subclasses of receptors classified according to their sequence homologies and their binding affinity for ephrins (Eph receptor interacting protein).[17,18] Targeting of EphA2 receptor using monoclonal antibodies for tumor growth inhibition has been demonstrated in EphA2 overexpressing prostate and ovarian cancers.[19] However, delivery of anticancer drug loaded liposome targeting EphA2 receptor for treatment of lung cancer has not been investigated. EphA2 expression in lung, colon, skin, and kidney was over 10-fold higher relative to the bone marrow, which could be helpful in minimizing the myelosuppresive toxicity of EphA2 targeted anticancer nanocarriers.[19] Moreover, the highest level of EphA2 is observed in clinically advanced stages of lung cancer.[18,19] Recently, an ephrin mimicking amino acid sequence (YSA; YSAYPDSVPMMS) is a peptide identified to selectively target EphA2 receptor activation and cellular internalization.[20,21]

Collagen and hyaluronic acid rich dense extracellular matrix of solid tumor severely compromises the uptake of nano-carriers.[22,23] However, the EPR effect mediated passive targeting and tumor antigen directed active targeting are the commonly used strategies for targeting tumor, but extensive fibrosis of tumors (e.g., pancreatic, breast) restricts the clinical efficiency of nanocarriers. Reduction in tumor fibrosis by stromal disruption could be a promising strategy to augment the anticancer effect of nanomedicines. There are few reports demonstrating the use of collagenase, hyaluronidase, and lysyl oxidase to enhance delivery of therapeutics by degrading tumor ECM.[24–27] However, orally bioavailable small molecule inhibitor could be preferred over intravenous proteolytic enzymes for this purpose. Researchers have shown enhanced uptake of antibody, virus, or nanocarriers in tumors by disrupting tumor stroma using bacterial collagenase, relaxin, or transforming growth factor beta (TGF-β1) inhibitors.[23,26,28,29] Telmisartan is an angiotensin receptor (AT) blocker used for the treatment of hypertension. In our previous report we have demonstrated that telmisartan led to significant reduction in collagen-I content in lung tumors and increased the uptake of fluorescent nanoparticles compared to control group.[30] In these studies, we administered telmisartan by inhalation route. Further, we also demonstrated that inhibition of TGF-β1 was one of the major mechanisms involved in antifibrotic activity of inhalable telmisartan in lung tumors. However, these studies were limited to fluorescent nontargeted

nanoparticles, and we have not evaluated anticancer efficacy of any chemotherapeutic agent loaded nanoparticles. The current paper demonstrates the preclinical application of this approach by investigating the role of oral telmisartan treatment mediated degradation of tumor extracellular matrix in enhancing the efficacy of actively targeted nanoliposomes.

The objectives of this study in an effort to further explore the translational outcomes of our approach are (1) to develop and optimize YSA anchored PEGylated nanoliposomes of docetaxel (YDPL) using modified hydration method, (2) to evaluate the effect of oral telmisartan mediated compromised tumor barrier on the anticancer efficacy of YDPL in orthotopic lung cancer bearing mice, and (3) investigation of cellular uptake mechanism of YDPL.

EXPERIMENTAL SECTION

Chemicals and Drugs

Docetaxel was purchased from AK Scientific (Union City, CA, USA). Phospholipids were purchased from Lipoid (Germany). All other chemicals and HPLC solvents were purchased from Sigma-Aldrich (St. Louis, MO). DMEM-F12K medium, fetal bovine serum, and other cell culture materials were purchased from Lonza (Basel, Switzerland). Primary antibodies were purchased from cell signaling technology (USA). 1,2-Dioleoyl-*sn*-glycero-3-[(*N*-(5-amino-1-carboxypentyl) imidodiacetic acid) succinyl nickel salt] (DOGS-NTA-Ni) was purchased from Avanti Polar Lipids (Alabaster, AL, USA). The six histidine tagged PEGylated YSA (6His-PEG-YSA) tumor homing peptide and control nonspecific peptide YKA (6His-PEG-YKA) peptide were synthesized by GenScript Corporation (Piscataway, NJ, USA). Chlorpromazine, MβCD, genistein, amantadine, nocodazole, hydroxychloroquine and amiloride were purchased from Santa Cruz Biotechnology, Santa Cruz, CA, USA.

HPLC Analysis

Reverse phase HPLC-UV method was used to analyze DTX. Chromatographic separation was achieved on Waters 717 instrument equipped with waters symmetry (250 mm/4.6 mm/5 μm) column using ACN:phosphate buffer pH 3 (55:45) as mobile phase with flow rate of 0.55 mL/min, detected at 227 nm.

Animals

Female, 6-week old, athymic Nu/nu mice were purchased from Harlan Inc. (Indianapolis, IN). The mice were housed and maintained in specific pathogen-free conditions in a facility approved by the American Association for Accreditation of Laboratory Animal Care. Food and water were provided ad libitum to the animals in standard cages. Animals were maintained at standard conditions of 37 °C and 60% humidity. All experiments were done in accordance with the guidelines of the Institutional Animal Care and Use Committee (IACUC) at Florida A&M University. Animals were acclimatized for 1 week prior to the tumor studies.

Preparation of YSA Anchored PEGylated Liposomes

Docetaxel (DTX) loaded PEGylated liposomes (DPL) and YSA anchored DTX loaded PEGylated liposomes (YDPL) were prepared using a modified hydration method. Briefly, DTX:DOGS-NTA-Ni:DOPC:cholesterol:DSPE-PEG 2000 in a 0.5:5:20:5:2.5 weight ratio were dissolved in chloroform. The solution was dropwise added to mannitol at 45 °C with constant stirring in glass mortar and pestle and left overnight in an oven (37 °C) for evaporation of residual chloroform. Resultant powder was dispersed into water (50 °C) using a cyclomixer followed by sonication for 4 min using a probe sonicator at 30% amplitude (Branson probe sonicator, 400 W, USA). Mannitol and unentrapped DTX were separated by passing the liposomes through a Sephadex G50 column. DTX was prepared using the same formula as the marketed DTX formulation, Taxotere (Sanofi-Aventis, USA). YSA solution (10 mg/mL) was prepared in water and appropriately added into prepared liposomes to achieve various DOGS-NTA-Ni:YSA molar ratios. The mixture was incubated for 30 min. Coumarin-6 loaded PEGylated liposomes (C6PL) and YSA anchored coumarin-6 loaded PEGylated liposomes (YC6PL) were prepared using the same method by replacing DTX with coumarin-6.

The effect of YSA concentration on particle size and zeta potential was evaluated. YSA binding was evaluated by BCA protein estimation kit (Thermoscientific, USA). Briefly, 500 μL of YSA coated liposomes was filled into Amicon Ultra centrifugal filters (30 kDa) (Millipore, Ireland) and free YSA was separated by centrifuging the samples at 10,000 rpm for 10 min. Concentration of free YSA was analyzed using a BCA protein estimation kit.

$$\%\text{YSA binding} = \frac{\text{amount of YSA attached to liposomes}}{\text{total YSA added}} \times 100$$

Particle Size, Zeta Potential, and Entrapment Efficiency

Hydrodynamic diameter of formulation was analyzed by dynamic light scattering (DLS) using Nicomp PSS particle size analyzer (PSS Systems, USA). Formulation was diluted into HPLC grade water to achieve concentration of 0.1 mg/mL of DTX. Entrapment efficiency was analyzed using gel permeation chromatography using a Sephadex G50 column (Sigma-Aldrich, USA).

Flow Cytometry Analysis

Cellular uptake of C6PL and YC6PL was evaluated in lung adenocarcinoma cell line (A549) using flow cytometry. A549 cells were seeded in a 6-well plate at a density of 3×10^5 cells/well and incubated in 1 mL of complete growth medium. After 24 h, cells were washed with HBSS and incubated with C6PL or YC6PL in HBSS for 30 min. To evaluate the specificity of EphA2 receptor specific uptake, free YSA peptide (50 times higher amount than present on the surface of YC6PL) was added. After 30 min of incubation, cells were thoroughly washed with HBSS, trypsinized, and collected in a tube for FACS analysis. The intracellular fluorescence of C6 was determined using a fluorescence-activated cell sorter (FACS, Calibur flow cytometer, BD, Franklin Lakes, NJ, USA).

Cellular Uptake Mechanism

Various pharmacological and physical inhibitors were used to investigate the cellular uptake mechanism of YDPL.[31,32] A549 cells were seeded in a 96-well plate at a density of 10,000 cells/well and incubated for 24 h in DMEM-F12K medium. After 24 h, cells were washed with HBSS and incubated with various endocytosis inhibitors for 2 h ($n = 12$). Chlorpromazine (20 μM) and amnatadine (2 mM) were used to inhibit the clathrin dependent endocytosis while methyl-β-cyclodextrin (MβCD-5 mM) and genistein (50 μM) were used as caveolae dependent endocytosis inhibitors. Amiloride (50 μM) was used to block macropinocytosis. Hydroxychloroquine sulfate (HCQ-20 μM) was added to evaluate the role of endosomal escape in YC6PL uptake while nocodazole was used as inhibitor of microtubule cytoskeleton. After 2 h of incubation with this inhibitor, YC6PL was added in well to achieve 1 μg/mL C6 concentration in well. To evaluate EphA2 receptor specific uptake of YC6PL, free YSA peptide (50 times higher amount than present on the surface of YC6PL) was added in one of the samples. In order to determine whether YC6PL uptake was an active or passive process, YC6PL treated cells were also incubated at 4 °C.

After 30 min of exposure of YC6PL, cells were thoroughly washed with HBSS and observed with fluorescence microscope (Olympus Instruments, USA). Intensity of green color as a measurement of coumarin-6 uptake was carried out using ImageJ software. Percentage change in average fluorescence intensity with respect to YC6PL group was plotted.

Inoculation of A549 in Mice

A549 cells were grown in DMEM-F12K medium containing 10% FBS and standard antibiotic mix at 5% CO_2 and 37 °C. For orthotopic lung tumor model, mice were anesthetized with isoflurane and a 5 mm skin incision was made to the left chest, 5 mm below the scapula.[1,33,34] Hamilton syringe with 28-gauge hypodermic needles was used to inject A549 cells through the sixth intercostal space into the left lung. The needle was quickly advanced to a depth of 3 mm and removed after the injection of the cells (2 million per mouse) suspended in 100 μL of PBS (pH 7.4) into the lung parenchyma. Wounds from the incisions were closed with surgical skin clips. Animals were observed for 45 to 60 min until fully recovered. The animals develop lung tumor within 14 days after the cell inoculation.[2,3,35]

Antitumor Study

After 14 days, animals were randomly divided into five groups (saline solution, DTX, DTXPL, YDPL and YDPL + telmisartan) of 12 animals each. Telmisartan treatment was started on the15th day of cell inoculation while DTX treatment was started from the 17th day. The dose of DTX (intravenous) and telmisartan (oral) was 5 mg/kg body weight. Six doses of DTX formulations were given biweekly for 3 weeks. Two doses of telmisartan were given at 24 and 48 h before each DTX dose. Animals were sacrificed, 3 days after the last dose of DTX formulation. Lungs were collected, weighted, and observed for lung tumor growth using a stereomicroscope (Olympus, USA). The same tumors were used for immunohistochemistry (IHC) and Western blot analysis.

Coumarin-6 Liposome Uptake in Lung Tumor

After 21 days of A549 inoculation, animals were divided into two groups: control and telmisartan. The control group received saline solution and the telmisartan group received 2 doses of telmisartan (5 mg/kg, once a day) by the oral route (22nd and 23rd days). On the 24th day, intravenous injection of YC6PL (1 mg/kg) was given in both groups via tail vein. Animals were sacrificed after 1 h, and lungs were collected. Cryosection (40 μm thickness) of the part of lung bearing tumor nodules was carried out and immediately observed with the Olympus fluorescent microscope. Intensity of green color as a measurement of coumarin-6 uptake in normal lung and tumor tissue was carried out using ImageJ software.

Western Blot Analysis

To analyze the expression of different proteins in tumor samples, protein lysates of tumor tissues were prepared by using RIPA lysis buffer.[36] RIPA lysis buffer contains protease inhibitors and 500 mM phenyl methyl sulfonyl fluoride (PMSF). Concentration of protein in different samples was measured by using BCA protein assay reagent kit. Equal amounts of protein (50 μg) from each sample were denatured by heating for 5 min in SDS sample buffer. Protein samples were separated by 10% SDS-PAGE and then transferred to nitrocellulose membranes for immunoblotting. Membranes were blocked with skim milk (5% skim milk in 10 mM Tris-HCl (pH 7.6), 150 mM NaCl, and 0.5% Tween 20) three times and further probed with respective primary antibodies overnight at 4 °C. The primary antibodies such as MMP-9, TIMP-1, E-cadherin, Snail, Col1A, and β-actin were used in 1:1000 dilutions. HRP-conjugated specific secondary antibodies were used against primary antibodies. The detailed procedure for Western blotting was followed according to our published methods.

Immunohistochemistry of EphA2 and PCNA Expression

The expression of EphA2 and proliferated cell nuclear antigen (PCNA) were examined by immunohistochemistry using collected tumor samples of different groups. Paraffin-embedded tumor tissues were deparaffinized and blocked for peroxidase activity for EphA2 and PCNA expression. The specimens were washed with PBS twice and then blocked with normal goat serum according to the manufacturer's instructions (Santa Cruz Biotechnology, Santa Cruz, CA, USA). Subsequently, the sections were incubated with EphA2 and PCNA antibodies, at 4 °C overnight, followed by a 30 min treatment with HRP secondary antibody (Santa Cruz Biotechnology, Santa Cruz, CA, USA). After three washes with PBS, the sections were developed with diaminobenzidene-hydrogen peroxidase substrate and the counterstaining was done with hematoxylin. Finally, permanent mounting medium was applied to the slides, which were then mounted with glass coverslips, and images were taken with an Olympus microscope (Olympus Instruments, USA).

Statistics

All data are presented as the mean ± standard deviation (SD). The significance of difference in treatment groups was determined using Student's *t* test or one-way ANOVA using GraphPad prism version 5.0 (San Diego, CA), where a value of $p < 0.05$ between the groups was considered as a statistically significant difference between these groups.

RESULTS

Formulation Development and Characterization

DPL was prepared by modified hydration method using mannitol as water-soluble inert carrier. Immediately after ultrasonication, mannitol was separated from liposomes by size exclusion chromatography. Addition of YSA peptide significantly affected the zeta potential while a marginal effect on particle size was observed (Figure 1 a,b). Zeta potential was drastically reduced from −23.22 mV to −3.64 mV on addition of 1:0.5 M DOGS-NTA-Ni:YSA. Surface complexation of YSA increased the zeta potential of liposomes in a concentration dependent manner. Thereafter, there was a slight decrease in zeta potential at higher ratios, e.g., 1:1 and 1:1.5. The hydrodynamic diameter of DPL after separation of mannitol was 189.3 ± 5.7 nm. However, particle size was nearly similar at all the DOGS-NTA-Ni:YSA ratios. There was a slight decline in particle size from 189.3 nm to around 160 nm after incubation with YSA (Figure 1b).

YSA Binding Assay

YSA concentration was optimized by evaluating the percent YSA binding on liposomal surface while keeping the DOGS-NTA-Ni concentration constant. Hexahistidine chain of YSA peptide was expected to form complex with Ni present on liposomal surface. Percentage YSA binding consistently decreased with increasing the DOGS-NTA-Ni:YSA ratio. The highest percentage of YSA binding, 96.14%, was observed at the lowest (1:0.25) molar ratio while 78.38% YSA was bound at a 1:0.5 molar ratio, which suggested that the free Ni site on liposomal surface was saturated (Figure 1c). Further addition of YSA over 1:0.5 molar ratio led to poor percent YSA binding of around 50%.

Cellular Uptake Studies

Cellular internalization of coumarin-6 fluorescent probe loaded liposomes in A549 cells was evaluated by FACS analysis. There was a significant rightward shift in fluorescence intensity in YC6PL compared to C6PL, indicated higher cellular uptake of YC6PL compared to non-YSA coated liposomes (Figure 2). The geo mean of fluorescent intensity was almost 2-fold higher in YC6PL. Additionally, there was a significant decrease in geo mean with leftward shift in fluorescence graph when YC6PL was coincubated with high concentration of free YSA. In vitro cellular uptake demonstrated that surface complexation with YSA peptide selectively increased the targeting to lung cancer cells.

Cellular Uptake Mechanism

The mechanism of cellular internalization and intracellular trafficking of YC6PL was investigated on the A549 cell line using various endocytosis and endosomal inhibitors. Intensity of green color directly corresponds to intracellular concentration of coumarin-6 loaded liposomes. Trivial to considerable changes in green fluorescence intensity in the perinuclear region of A549 cells were observed with various inhibitors. Figure 3 represents the internalization of YC6PL by A549 cells in the presence of inhibitors of clathrin- or caveolae-mediated uptake. Most importantly, YC6PL coincubated with free YSA peptide showed highest reduction in cellular uptake. This result was quite similar to geo-mean

values of flow cytometry analysis. Cellular uptake of YC6PL by A549 cells was through energy dependent endocytosis, as it was reduced by 38.59% when incubated at 4 °C (Figure 3). Pretreatment of the cells with caveolae dependent uptake inhibitors, genistein and MβCD, prior to incubation with the YC6PL showed the most prominent reduction in fluorescence intensity compared to other types of endocytosis blockers. There was no statistically significant difference observed between intensity of cells incubated at 4 °C and cells treated with genistein and MβCD ($p > 0.05$). However, chlorpromazine and amantadine, which are known to perturb clathrin-mediated endocytosis, caused marginal changes in the uptake of the YC6PL. Cells pretreated with amiloride (macropinocytosis blocker) and nocodazole (microtubule cytoskeleton inhibitor) showed <20% inhibition of YC6PL uptake. By contrast, HCQ pretreated cells showed 14% enhancement in fluorescence intensity.

Uptake of Coumarin-6 PEGylated Liposomes in Lung Tumor

YC6PL was injected to observe their distribution in normal lung versus tumor tissue. Cryosection of lungs of control and telmisartan treated animals are shown in Figure 4. Intensity of green fluorescence in normal lung tissue is nearly equal in both the groups, but it was significantly higher ($p < 0.05$) in tumors in the telmisartan treated group. Lung tissues bearing tumor nodule were sectioned in such a way that each section has tumor and healthy lung tissue part. The red arrow in Figure 4 indicates the tumor nodule part while the blue arrow indicates the healthy lung tissue. Normal lung tissues have porous structure due to alveoli while tumor tissue is solid and dense, a much less porous structure compared to healthy lung tissue.

Anticancer Study in Orthotopic Lung Tumor Bearing Nude Mice

As shown in Figure 5, lungs were completely covered with tumor growth in control group while partially covered in DTX and DPL treated groups. Interestingly, significant inhibition of tumor growth was observed in YDPL and YDPL + telmisartan treated group. Similar results were reflected in lung tumor weight analysis (Figure 5). Oral telmisartan did not show any inhibition of lung tumor growth (data not shown). Interestingly, average lung tumor weight of the YDPL + telmisartan treated group was 4.8- and 3.8-fold lower than that of the DPL and YDPL treated groups ($p < 0.05$). Moreover, lung integrity was mostly intact and regular.

IHC analysis of tumor samples collected from various treatment groups revealed that expression of EphA2 and proliferation marker-PCNA were significantly downregulated ($p < 0.05$) with DTX liposomal treatment (Figure 6). Though there is no noticeable difference in expression of aforesaid markers in YDPL and YDPL + telmisartan treated groups, both groups differ significantly from the DPL group. The results of IHC for PCNA marker can be correlated with in vivo efficacy data, where the YDPL + telmisartan group showed nearly complete inhibition of lung tumor growth.

Western blot analysis of protein lysates isolated from lung tumor samples of various treatment groups is depicted in Figure 7. Western blot analysis further confirmed the superior anticancer and antifibrotic effects of YDPL + telmisartan compared to YDPL alone

and DPL. Levels of MMP9 and Snail were found to be significantly lower ($p < 0.05$) in combination treated group which suggested the metastasis inhibitory effect of formulation while upregulation E-cadherin is an indicator of the tumor suppressive effect. Interestingly, Snail showed similar expression in all other treatment groups except YDPL + telmisartan ($p < 0.01$). E-cadherin and, most importantly, significant reduction in the expression of Col 1A (marker for type I collagen) were observed in the combination group.

DISCUSSION

Tumor targeted nanocarriers constitute an important modality for the selective delivery of chemotherapeutics as they are capable of delivering a highly potent dose to the tumor site while minimizing off target side effects.[5,37] Enhanced permeation and retention (EPR) effect helps in passive targeting, but further penetration into tumors is minimized by the stromal barriers. Extracellular matrix rigidity due to dense collagen-I network in solid tumor leads to decreased convection and trans-capillary transport of anticancer drugs and nanocarriers to deep tumor regions.[8,22,23] Long plasma circulation and active targeting are not enough to deliver the drug to deeper layers of the tumors. This is the first report demonstrating the role of tumor stromal disruption in anticancer efficacy of targeted nanocarriers. Development of long circulating DTX liposomes with extended stability profile is a very challenging task. Here, we formulated DTX loaded PEGylated liposomes (DPL) using a modified hydration method developed in our laboratory. Further, there is no previous report investigating the pharmacodynamics profile of targeted PEGylated liposomal DTX against lung tumor xenografts. Tethering of YSA peptide on the DPL surface was expected to promote internalization in lung cancer cells via interaction with EphA2 receptors. In the present study, YSA coated PEGylated nanoliposomes of DTX (YDPL) were prepared, characterized, and evaluated in orthotopic lung tumor xenografts in athymic nude mice with and without prior treatment with oral antifibrotic agent, telmisartan.

In the thin film hydration method, drug–phospholipid film is formed in a round-bottom flask or glass beads and hydrated for 45 min to 1 h on a rotary evaporator. In the modified hydration method, the drug-lipid film is prepared over mannitol microparticles and hydrated within 1 min. We have prepared the DPL batches with both methods with the same composition. The DPL batches prepared using thin film hydration were physically stable for 10–12 h only while with modified hydration method DPL batches were stable for 2 weeks at room temperature. There was 7–8-fold enhancement in physical stability with the modified hydration method.

DPL was prepared using a nickel-chelating lipid (1,2-dioleoyl-*sn*-glycero-3-[*N*-(5-amino-1-carboxypentyl)-iminodiacetic acid] succinyl (nickel salt) (DOGS-NTA-Ni)) to allow surface complexation of His-tagged targeting ligand. His-tagged YSA peptide was added in different concentrations to optimize the particle size, zeta potential, and YSA binding. We have preferred this technique over chemical conjugation of YSA on liposomal surface, which is more tedious. Gradual rise in zeta potential was observed with increasing YSA concentration while particle size was largely unaffected. Surface complexation of YSA increased the zeta potential of liposomes in a concentration dependent manner except at higher concentrations. Succinyl group of DOGS-NTA-Ni are responsible for negative zeta

potential of DPL. Complexation of Ni with YSA peptide could have resulted in masking of anionic charge and shifting the zeta potential toward 0. At higher ratio, 1:1 and 1:1.5, the DPL surface became saturated with YSA, and therefore, no more increment in zeta potential was observed. The same behavior was observed in percent YSA binding study. Therefore, a DOGS-NTA-Ni:YSA molar ratio of 1:0.5 was optimized for YDPL.

Bally et al., 2002, have extensively investigated the effect of mole percentage of DOGS-NTA-Ni and DSPE PEG 2000 on the binding and stability of poly histidine tagged peptides on liposomal surface.[38] They have suggested that 5 mol % of DOGS-NTA-Ni gave optimum binding while surface PEGylation reduced the rate of binding but not the overall efficiency of binding. A similar approach has been used by Altin et al., 2011, for targeting dendritic cells. Histidine-tagged peptides derived from ICAM4 (intercellular cell adhesion molecule 4) and synthetic high-mobility group box 1 (HMGB1) mimicking peptide were conjugated to Ni-NTA3-DTDA functionalized liposomes for targeting dendritic cells to improve the immunogenicity.[39,40] In another report, pyropheophorbide α loaded lipid nanoparticles containing DOGS-NTA-Ni was synthesized as platform theranostic technology for imaging and treatment of various cancers using suitable peptides.[41]

Cellular uptake studies revealed that YSA complexation led to significant enhancement in uptake of C6PL liposomes. Moreover, reduction in the uptake of YC6PL on coincubation with free YSA peptide confirmed the EphA2 receptor specific uptake of YC6PL. EphA2 receptor targeting in brain, lung, prostate, and breast cancer cells using YSA conjugated anticancer drugs or YSA anchored nanoparticles (solid lipid nanoparticle and liposomes) has been demonstrated by various groups.[17,20,21,41–44] However, there has been no consensus about cellular uptake mechanism of YSA anchored nano-particles. Endocytosis is the major route for the transportation of nanomedicines across the cell membrane. Usually nano-particles are internalized by clathrin and caveolae dependent endocytosis, macropinocytosis, and clathrin or caveolae independent endocytosis depending on the surface characteristics of nanoparticles.[31,32,45] Endocytosis inhibitors are used to investigate the uptake pathway. As most of the endocytic pathways are energy dependent, they can be inhibited by low temperature. Results of cellular uptake mechanism study demonstrated that low temperature led to significant reduction in uptake of YC6PL. Similar behavior was observed for YC6PL incubated with free YSA. This suggests that internalization of YDPL is energy dependent and EphA2 receptor specific. Chlorpromazine and amantadine are inhibitors of clathrin-coated pit formation which marginally decreased the YC6PL uptake to <20% compared to YDPL alone. Caveolae inhibitors, genistein and MβCD, showed considerable reduction in the uptake of YC6PL, suggesting that caveolae-mediated endocytosis was more important for the uptake of YDPL than clathrin-dependent uptake and macropinocytosis.[45] Caveolae-mediated endocytosis involves clustering of lipid raft components on the plasma membrane into flask-shaped invaginations. MβCD is a cyclic oligomer of glucopyranoside that inhibits cholesterol dependent endocytic processes by reversibly extracting the steroid out of the plasma membrane. Genistein is a tyrosine-kinase inhibitor that causes disruption of the actin network at the endocytosis site and inhibits the recruitment of dynamin II, both known to be essential events in the caveolae-mediated uptake mechanism.[32,45] Interestingly, enhancement in fluorescence in the endosome lytic agent pretreated group demonstrated that the EphA2

receptor internalization pathway involves the classic endolysosomal route to deliver cargo in the intracellular milieu.[46]

Several preclinical studies suggest that active targeting improves antitumor efficacy as a result of enhanced cellular internalization of cytotoxic agents, rather than increased tumor accumulation.[22,47] Collagen, hyaluronic acid, and other proteins collectively make the tumor extracellular matrix less permeable to macromolecules and nanocarriers.[23] The restrictive tumor microenvironment can be normalized by pretreatment of agents that promote the degradation of extracellular matrix component. In our previous report we have shown that inhalable telmisartan reduced the expression of collagen-1, transforming growth factor beta 1 (TGF-β1), cleaved caspase-3, and vimentin expression in orthotopic lung tumors.[30] Since the oral route has very high patient compliance over the aerosol based inhalation route, in the present study telmisartan was administered by the oral route. Higher uptake of YC6PL can be correlated with the compromised tumor barrier due to TGFβ inhibition mediated disruption of collagen network by oral telmisartan treatment. Intensity of green fluorescence was much stronger in the tumor region of the telmisartan treated group. Distribution of YC6PL between healthy and tumorous lung tissues was nearly equal in the control group while tumor tissue favorable distribution of YC6PL was observed in the telmisartan treated group. This strategy allows not only enhanced delivery of nanoparticle therapeutics but also decreased toxicity to nontumor tissue sites. At the clinical level, this could be helpful in escalating dose and efficacy without increasing the toxicity to the patient.

Tumor stromal disruption and active targeting have synergistically contributed to anticancer efficacy of YDPL. There was not much difference in lung tumor weights of the DPL and YDPL groups, which might be due to similar amount of uptake of both the liposomes due to the EPR effect. Since YDPL is actively targeted to overexpressed EphA2 receptors of lung tumors, it has facilitated the higher intracellular delivery of DTX molecules. Once internalized, DTX is no longer available to diffuse back into systemic circulation. Thus, YDPL showed superior anticancer efficacy compared to DPL by delivering high payload to individual cells. However, YDPL can only enhance the cellular internalization of nanocarrier in lung cancer cells but does not help with deeper penetration of DTX into the solid tumor mass. As demonstrated by our research group in earlier study, tumoral uptake of liposomes was successfully augmented by pretreatment with telmisartan.[30]

Markers representing tumor fibrosis and epithelial-mesen-chymal transition (EMT) were studied by Western blot analysis. Significantly lower expression of collagen I in the combination group confirmed stromal disruption. Our studies suggest that the YDPL + telmisartan group inhibited the EMT process more efficiently by downregulating Snail and upregulating the E-cadherin levels. Tumor collagen modulates E-cadherin mediated cell-to-cell contact to increase tumor invasiveness and metastases. The decreased MMP9 and increased TIMP-1 levels further support the prominent antifibrotic effects of YDPL + telmisartan because MMP9 is one of the crucial components of extracellular matrix and is also involved in tumor fibrosis. Further our results were supported by immunohistochemistry data, which revealed substantial downregulation of EphA2 receptors and proliferating cell nuclear antigen (PCNA) expression in the YDPL and YDPL + telmisartan groups compared

to control. However, there was no significant difference observed between the YDPL and YDPL + telmisartan groups in IHC.

The normal tissues have low EphA2 expression compared to tumor tissues, and therefore use of the YSA peptide anchored nanocarrier for drug delivery may reduce off target side effects by reducing exposure of cytotoxic drugs to normal cells.[19] There are several clinical limitations to the use of monoclonal antibodies as a targeting moiety which can be overcome by using a receptor specific peptide. Physicochemical stability, formulation issues, risk of adverse immune reaction, and high manufacturing costs discourage use of monoclonal antibody over peptides. Scarberry et al. have reported the use of YSA peptide coated magnetic cobalt ferrite nanoparticles to target EphA2 expressing ovarian carcinoma cells.[42] Furthermore, an ephrinA1 conjugated *Pseudomonas aeruginosa* exotoxin A showed dose dependent killing of glioblastoma multiforme (GBM) cells at doses as low as 0.01 nM.[44] Similarly, Wang et al., 2013, showed that YSA-paclitaxel conjugate delivered significantly higher dose of paclitaxel to prostate tumors and was more effective in inhibiting tumor growth in prostate cancer xenografts in athymic nude mice.[20] However, YSA-drug conjugation is a complex and very expensive process with poor drug loading. Moreover, considering the constraints in parenteral delivery of taxanes, high dose, and plasma stability, YSA conjugated paclitaxel is not a feasible option for clinical applications. YSA anchored nanocarrier with high taxane loading could be a more promising approach in using EphA2 receptor directed delivery. YSA anchored nanocarrier can deliver a large pay load of drug with same amount of YSA compared to YSA–drug conjugate. In this case, PEGylated liposomes with surface anchored YSA peptide could be a simple, stable, and economical alternative to drug–peptide conjugate.

Current approach of compromising tumor barriers followed by active tumor targeting can be applicable to many other solid tumors for enhancing nanoparticle delivery and distribution. Since there are some nanomedicinal products available on the market and many of them in clinical trials including nanocarriers for delivering DNA, siRNA, diagnostic agents, or imaging agents, pretreatment with oral telmisartan could be of great significance in enhancing the tumoral delivery of all these nanocarriers.

Supplementary Material

Refer to Web version on PubMed Central for supplementary material.

Acknowledgments

This research was supported with funding from the National Institutes of Health’s Minority Biomedical Research Support (MBRS)-SC1 program [Grant # SC1 GM092779-01], Cancer Institute of the National Institutes of Health under Award Number R21CA175618, and the National Institute on Minority Health and Health Disparities (NIMHD) P20 program [Grant # 1P20 MD006738-03].

References

1. Fulzele SV, Chatterjee A, Shaik MS, Jackson T, Ichite N, Singh M. 15-Deoxy-Delta12,14-prostaglandin J2 enhances docetaxel anti-tumor activity against A549 and H460 non-small-cell lung cancer cell lines and xenograft tumors. Anti-Cancer Drugs. 2007; 18(1):65–78. [PubMed: 17159504]

2. Fulzele SV, Chatterjee A, Shaik MS, Jackson T, Singh M. Inhalation delivery and anti-tumor activity of celecoxib in human orthotopic non-small cell lung cancer xenograft model. Pharm. Res. 2006; 23(9):2094–106. [PubMed: 16902813]

3. Ichite N, Chougule MB, Jackson T, Fulzele SV, Safe S, Singh M. Enhancement of docetaxel anticancer activity by a novel diindolylmethane compound in human non-small cell lung cancer. Clin. Cancer Res. 2009; 15(2):543–52. [PubMed: 19147759]

4. Al-Abd AM, Aljehani ZK, Gazzaz RW, Fakhri SH, Jabbad AH, Alahdal AM, Torchilin VP. Pharmacokinetic strategies to improve drug penetration and entrapment within solid tumors. J. Controlled Release. 2015; 219:269–77.

5. Bae YH, Park K. Targeted drug delivery to tumors: myths, reality and possibility. J. Controlled Release. 2011; 153(3):198–205.

6. Jain RK, Stylianopoulos T. Delivering nanomedicine to solid tumors. Nat. Rev. Clin. Oncol. 2010; 7(11):653–64. [PubMed: 20838415]

7. Lammers T, Kiessling F, Hennink WE, Storm G. Drug targeting to tumors: principles, pitfalls and (pre-) clinical progress. J. Controlled Release. 2012; 161(2):175–87.

8. Kobayashi H, Watanabe R, Choyke PL. Improving conventional enhanced permeability and retention (EPR) effects; what is the appropriate target? Theranostics. 2014; 4(1):81–9.

9. Doddapaneni R, Patel K, Owaid IH, Singh M. Tumor neovasculature-targeted cationic PEGylated liposomes of gambogic acid for the treatment of triple-negative breast cancer. Drug Delivery. 2016:1–10. [PubMed: 24758139]

10. Nag OK, Awasthi V. Surface engineering of liposomes for stealth behavior. Pharmaceutics. 2013; 5(4):542–69. [PubMed: 24300562]

11. Chang HI, Yeh MK. Clinical development of liposome-based drugs: formulation, characterization, and therapeutic efficacy. Int. J. Nanomed. 2012; 7:49–60.

12. Patel K, Patil A, Mehta M, Gota V, Vavia P. Medium chain triglyceride (MCT) rich, paclitaxel loaded self nanoemulsifying preconcentrate (PSNP): a safe and efficacious alternative to Taxol. J. Biomed. Nanotechnol. 2013; 9(12):1996–2006. [PubMed: 24266255]

13. Patel K, Patil A, Mehta M, Gota V, Vavia P. Oral delivery of paclitaxel nanocrystal (PNC) with a dual Pgp-CYP3A4 inhibitor: preparation, characterization and antitumor activity. Int. J. Pharm. 2014; 472(1–2):214–23. [PubMed: 24954663]

14. Molina JR, Yang P, Cassivi SD, Schild SE, Adjei AA. Non-small cell lung cancer: epidemiology, risk factors, treatment, and survivorship. Mayo Clin. Proc. 2008; 83(5):584–94. [PubMed: 18452692]

15. Brannan JM, Sen B, Saigal B, Prudkin L, Behrens C, Solis L, Dong W, Bekele BN, Wistuba I, Johnson FM. EphA2 in the early pathogenesis and progression of non-small cell lung cancer. Cancer Prev. Res. 2009; 2(12):1039–49.

16. Brannan JM, Dong W, Prudkin L, Behrens C, Lotan R, Bekele BN, Wistuba I, Johnson FM. Expression of the receptor tyrosine kinase EphA2 is increased in smokers and predicts poor survival in non-small cell lung cancer. Clin. Cancer Res. 2009; 15(13):4423–30. [PubMed: 19531623]

17. Patel AR, Chougule M, Singh M. EphA2 targeting pegylated nanocarrier drug delivery system for treatment of lung cancer. Pharm. Res. 2014; 31(10):2796–809. [PubMed: 24867421]

18. Xi HQ, Wu XS, Wei B, Chen L. Eph receptors and ephrins as targets for cancer therapy. J. Cell Mol. Med. 2012; 16(12):2894–909. [PubMed: 22862837]

19. Tandon M, Vemula SV, Mittal SK. Emerging strategies for EphA2 receptor targeting for cancer therapeutics. Expert Opin. Ther. Targets. 2011; 15(1):31–51. [PubMed: 21142802]

20. Wang S, Noberini R, Stebbins JL, Das S, Zhang Z, Wu B, Mitra S, Billet S, Fernandez A, Bhowmick NA, Kitada S, Pasquale EB, Fisher PB, Pellecchia M. Targeted delivery of paclitaxel to EphA2-expressing cancer cells. Clin. Cancer Res. 2013; 19(1):128–37. [PubMed: 23155185]

21. Wang S, Placzek WJ, Stebbins JL, Mitra S, Noberini R, Koolpe M, Zhang Z, Dahl R, Pasquale EB, Pellecchia M. Novel targeted system to deliver chemotherapeutic drugs to EphA2-expressing cancer cells. J. Med. Chem. 2012; 55(5):2427–36. [PubMed: 22329578]

22. Minchinton AI, Tannock IF. Drug penetration in solid tumours. Nat. Rev. Cancer. 2006; 6(8):583–92. [PubMed: 16862189]

23. Netti PA, Berk DA, Swartz MA, Grodzinsky AJ, Jain RK. Role of extracellular matrix assembly in interstitial transport in solid tumors. Cancer Res. 2000; 60(9):2497–503. [PubMed: 10811131]
24. Chauhan VP, Martin JD, Liu H, Lacorre DA, Jain SR, Kozin SV, Stylianopoulos T, Mousa AS, Han X, Adstamongkonkul P, Popovic Z, Huang P, Bawendi MG, Boucher Y, Jain RK. Angiotensin inhibition enhances drug delivery and potentiates chemotherapy by decompressing tumour blood vessels. Nat. Commun. 2013; 4:2516. [PubMed: 24084631]
25. Kanapathipillai M, Mammoto A, Mammoto T, Kang JH, Jiang E, Ghosh K, Korin N, Gibbs A, Mannix R, Ingber DE. Inhibition of mammary tumor growth using lysyl oxidase-targeting nanoparticles to modify extracellular matrix. Nano Lett. 2012; 12(6):3213–7. [PubMed: 22554317]
26. Murty S, Gilliland T, Qiao P, Tabtieng T, Higbee E, Al Zaki A, Pure E, Tsourkas A. Nanoparticles functionalized with collagenase exhibit improved tumor accumulation in a murine xenograft model. Part. Part. Syst. Charact. 2014; 31(12):1307–1312. [PubMed: 26380538]
27. Tredan O, Galmarini CM, Patel K, Tannock IF. Drug resistance and the solid tumor microenvironment. J. Natl. Cancer Inst. 2007; 99(19):1441–54. [PubMed: 17895480]
28. Cemazar M, Golzio M, Sersa G, Escoffre JM, Coer A, Vidic S, Teissie J. Hyaluronidase and collagenase increase the transfection efficiency of gene electrotransfer in various murine tumors. Hum. Gene Ther. 2012; 23(1):128–37. [PubMed: 21797718]
29. Guedan S, Rojas JJ, Gros A, Mercade E, Cascallo M, Alemany R. Hyaluronidase expression by an oncolytic adenovirus enhances its intratumoral spread and suppresses tumor growth. Mol. Ther. 2010; 18(7):1275–83. [PubMed: 20442708]
30. Godugu C, Patel AR, Doddapaneni R, Marepally S, Jackson T, Singh M. Inhalation delivery of Telmisartan enhances intratumoral distribution of nanoparticles in lung cancer models. J. Controlled Release. 2013; 172(1):86–95.
31. Xu S, Olenyuk BZ, Okamoto CT, Hamm-Alvarez SF. Targeting receptor-mediated endocytotic pathways with nanoparticles: rationale and advances. Adv. Drug Delivery Rev. 2013; 65(1):121–38.
32. dos Santos T, Varela J, Lynch I, Salvati A, Dawson KA. Effects of transport inhibitors on the cellular uptake of carboxylated polystyrene nanoparticles in different cell lines. PLoS One. 2011; 6(9):e24438. [PubMed: 21949717]
33. Chougule M, Patel AR, Sachdeva P, Jackson T, Singh M. Anticancer activity of Noscapine, an opioid alkaloid in combination with Cisplatin in human non-small cell lung cancer. Lung Cancer. 2011; 71(3):271–82. [PubMed: 20674069]
34. Ichite N, Chougule M, Patel AR, Jackson T, Safe S, Singh M. Inhalation delivery of a novel diindolylmethane derivative for the treatment of lung cancer. Mol. Cancer Ther. 2010; 9(11):3003–14. [PubMed: 20978159]
35. Jackson T, Chougule MB, Ichite N, Patlolla RR, Singh M. Antitumor activity of noscapine in human non-small cell lung cancer xenograft model. Cancer Chemother. Pharmacol. 2008; 63(1): 117–26. [PubMed: 18338172]
36. Patel K, Chowdhury N, Doddapaneni R, Boakye CH, Godugu C, Singh M. Piperlongumine for Enhancing Oral Bioavailability and Cytotoxicity of Docetaxel in Triple-Negative Breast Cancer. J. Pharm. Sci. 2015; 104(12):4417–26. [PubMed: 26372815]
37. Jin SE, Jin HE, Hong SS. Targeted delivery system of nanobiomaterials in anticancer therapy: from cells to clinics. BioMed Res. Int. 2014; 2014:814208. [PubMed: 24672796]
38. Chikh GG, Li WM, Schutze-Redelmeier MP, Meunier JC, Bally MB. Attaching histidine-tagged peptides and proteins to lipid-based carriers through use of metal-ion-chelating lipids. Biochim. Biophys. Acta, Biomembr. 2002; 1567(1–2):204–12.
39. Faham A, Altin JG. Ag-bearing liposomes engrafted with peptides that interact with CD11c/CD18 induce potent Ag-specific and antitumor immunity. Int. J. Cancer. 2011; 129(6):1391–403. [PubMed: 21128234]
40. Faham A, Bennett D, Altin JG. Liposomal Ag engrafted with peptides of sequence derived from HMGB1 induce potent Ag-specific and anti-tumour immunity. Vaccine. 2009; 27(42):5846–54. [PubMed: 19660589]

41. Anikeeva N, Sykulev Y, Delikatny EJ, Popov AV. Core-based lipid nanoparticles as a nanoplatform for delivery of near-infrared fluorescent imaging agents. Am. J. Nucl. Med. Mol. Imaging. 2014; 4(6):507–24. [PubMed: 25250201]

42. Scarberry KE, Dickerson EB, McDonald JF, Zhang ZJ. Magnetic nanoparticle-peptide conjugates for in vitro and in vivo targeting and extraction of cancer cells. J. Am. Chem. Soc. 2008; 130(31): 10258–62. [PubMed: 18611005]

43. Wang JL, Liu YL, Li Y, Dai WB, Guo ZM, Wang ZH, Zhang Q. EphA2 targeted doxorubicin stealth liposomes as a therapy system for choroidal neovascularization in rats. Invest. Ophthalmol. Visual Sci. 2012; 53(11):7348–57. [PubMed: 22977140]

44. Wykosky J, Gibo DM, Debinski W. A novel, potent, and specific ephrinA1-based cytotoxin against EphA2 receptor expressing tumor cells. Mol. Cancer Ther. 2007; 6(12):3208–18. [PubMed: 18089715]

45. Dutta D, Donaldson JG. Search for inhibitors of endocytosis: Intended specificity and unintended consequences. Cell Logist. 2012; 2(4):203–208. [PubMed: 23538558]

46. Shete HK, Prabhu RH, Patravale VB. Endosomal escape: a bottleneck in intracellular delivery. J. Nanosci. Nanotechnol. 2014; 14(1):460–74. [PubMed: 24730275]

47. Ruoslahti E, Bhatia SN, Sailor MJ. Targeting of drugs and nanoparticles to tumors. J. Cell Biol. 2010; 188(6):759–68. [PubMed: 20231381]

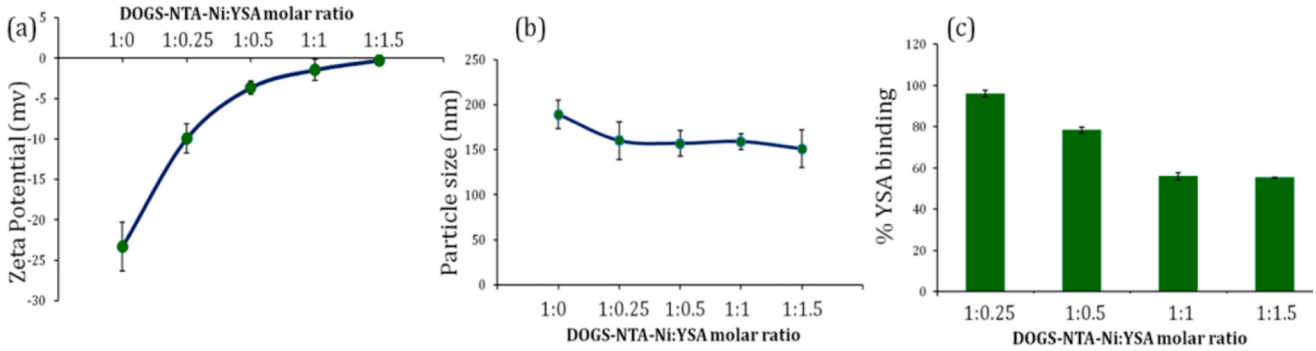

Figure 1.

Effect of YSA concentration on (a) zeta potential, (b) particle size, and (c) percentage of YSA binding on DTX loaded DOGS-NTA-Ni containing PEGylated liposomes (DPL). Data were given as mean ± SD (n = 3).

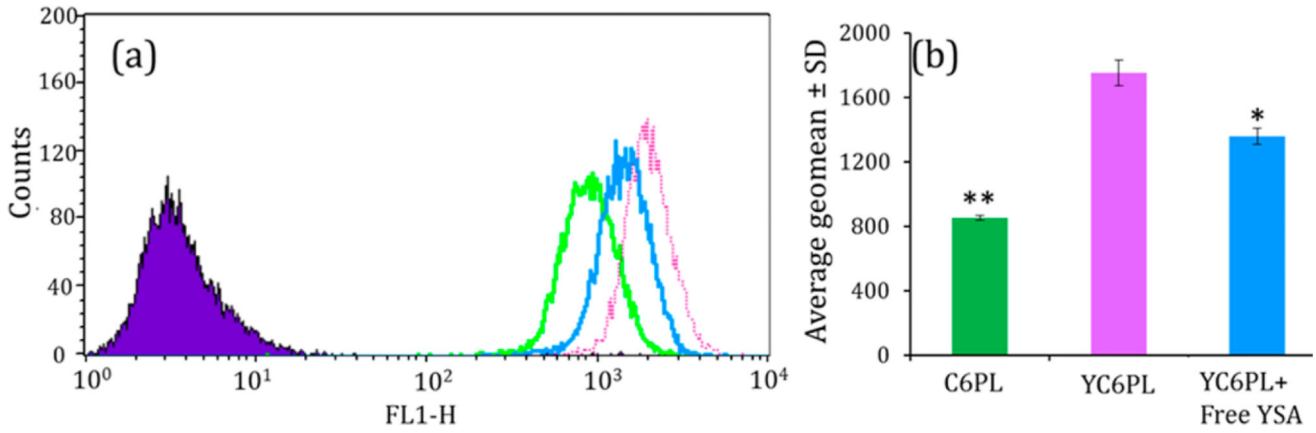

Figure 2.

Flow cytometry analysis of cellular uptake of C6PL and YC6PLwith or without free YSA peptide in A549 cells. (a) Flow cytometry histograms. (b) Average geo mean ± SD ($n = 6$). *$P < 0.05$, **$P < 0.01$. Significant enhancement in liposomal uptake was observed when surface coated with YSA peptide.

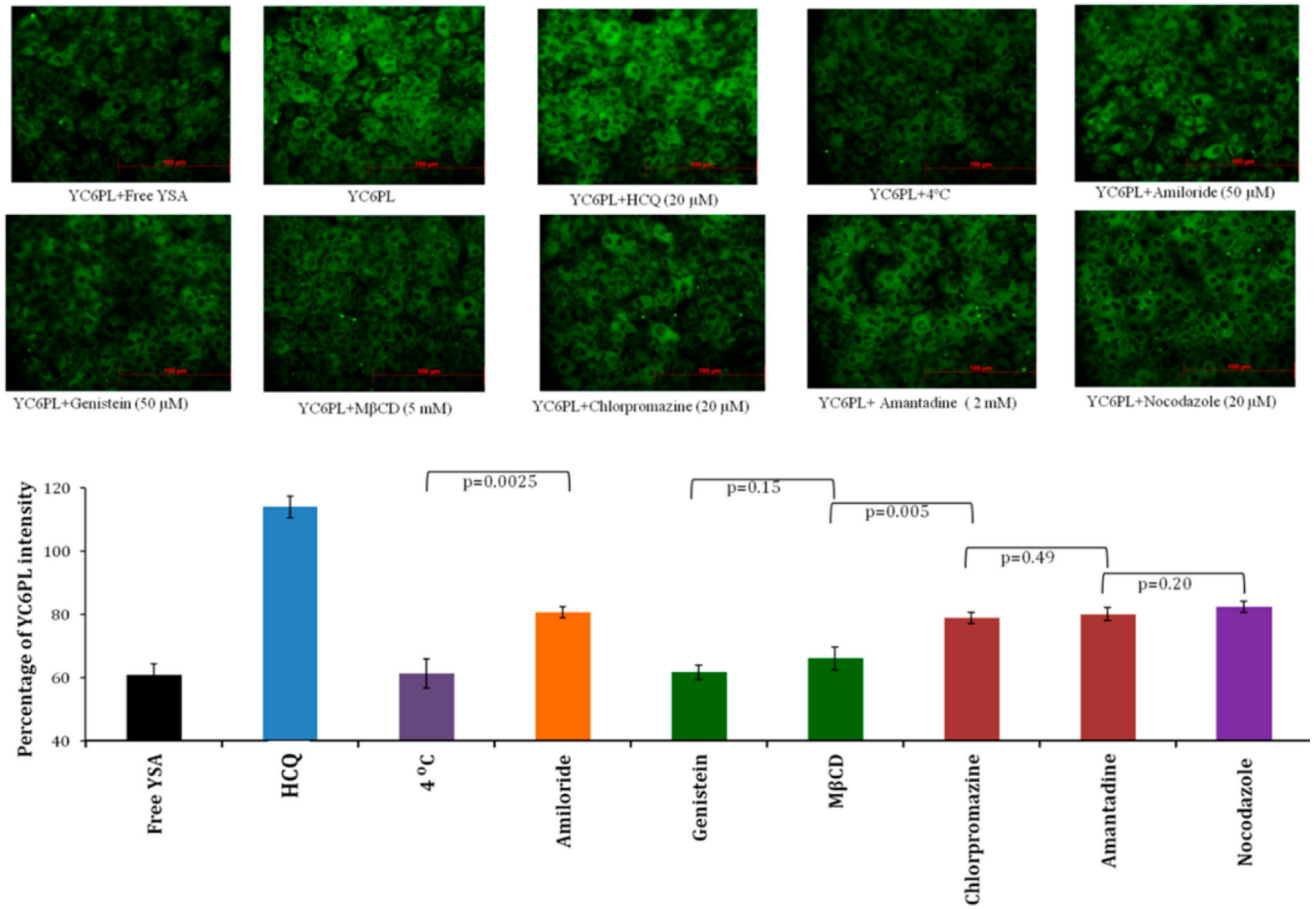

Figure 3.

Effect of endocytosis inhibitors on internalization of YC6PL in A549 cells. Cells were pretreated with HCQ, chlorpromazine, amantadine, genistein, nocodazole, and MβCD for 2 h before incubation with YC6PL for 30 min. Percentage intensity of green fluorescence (n = 12) compared to YC6PL treated cells was plotted. Pretreatment of the cells with caveolae dependent uptake inhibitors, genistein and MβCD, prior to incubation with the YC6PL showed most prominent reduction in fluorescence intensity compared to other types of endocytosis blockers.

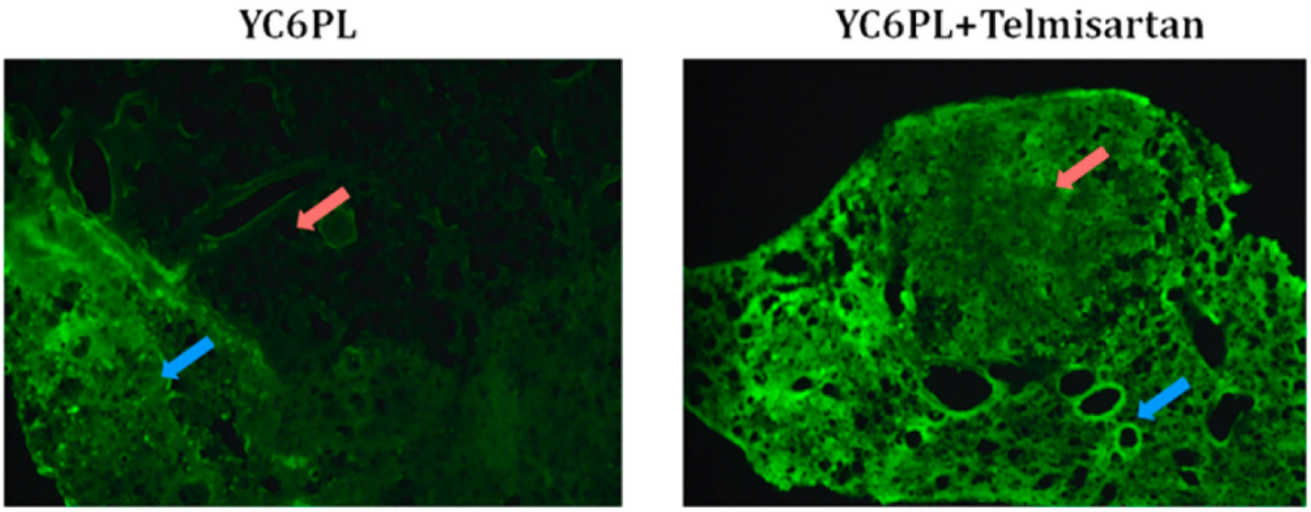

Figure 4.

Distribution of coumarin-6 liposomes in tumor bearing lung. Fluorescence images of lung sections of control and telmisartan treated animals. Red arrow indicates the tumor region while blue arrow indicates healthy lung tissue. Normal lung tissue showed similar fluorescence, but the telmisartan treated group showed higher fluorescence in tumor region as shown in graph.

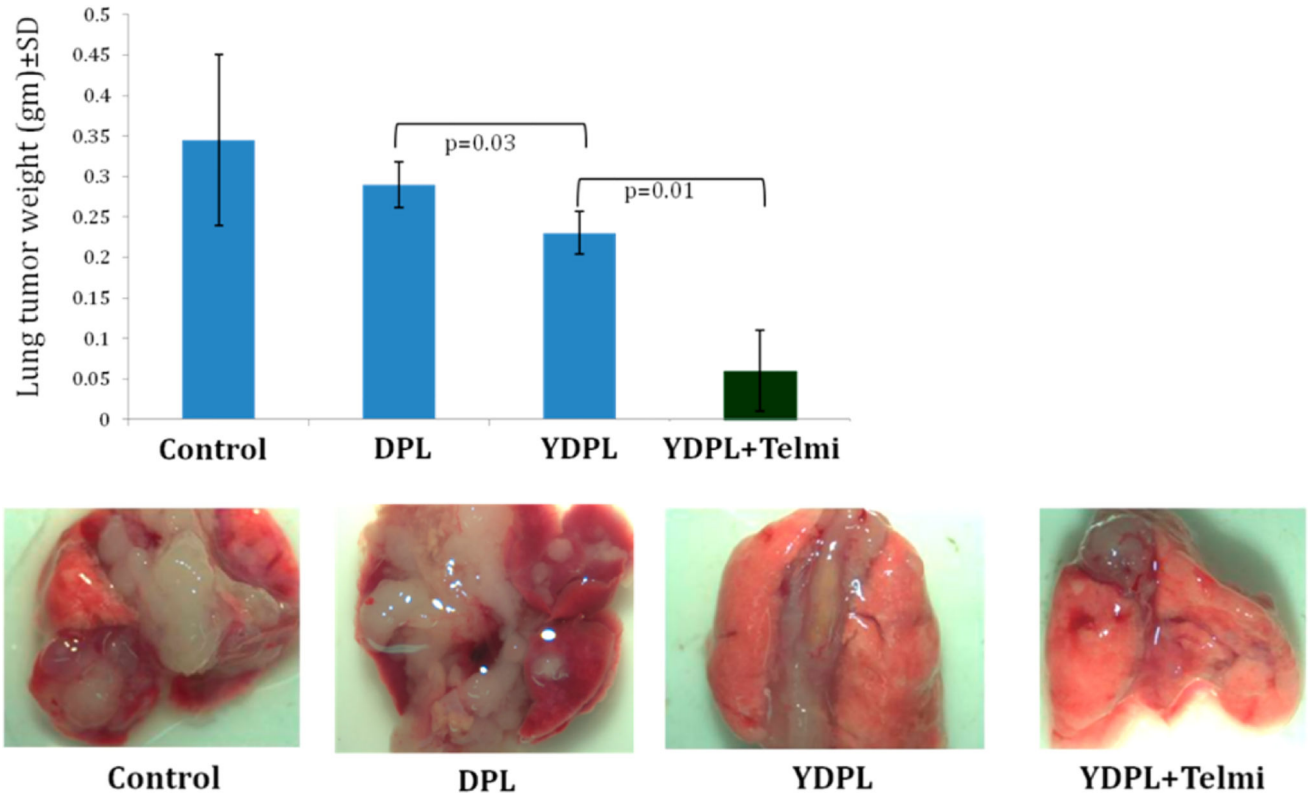

Figure 5.

In vivo anticancer efficacy study in A549 orthotopic lung tumor bearing nude mice. Lungs were collected 3 days after the last dose of DTX formulations. Lung tumor weight was significantly lower in the combination group with intact lung morphology as compared to other groups. Lung tumor weight data were given as mean ± SD (n = 12).

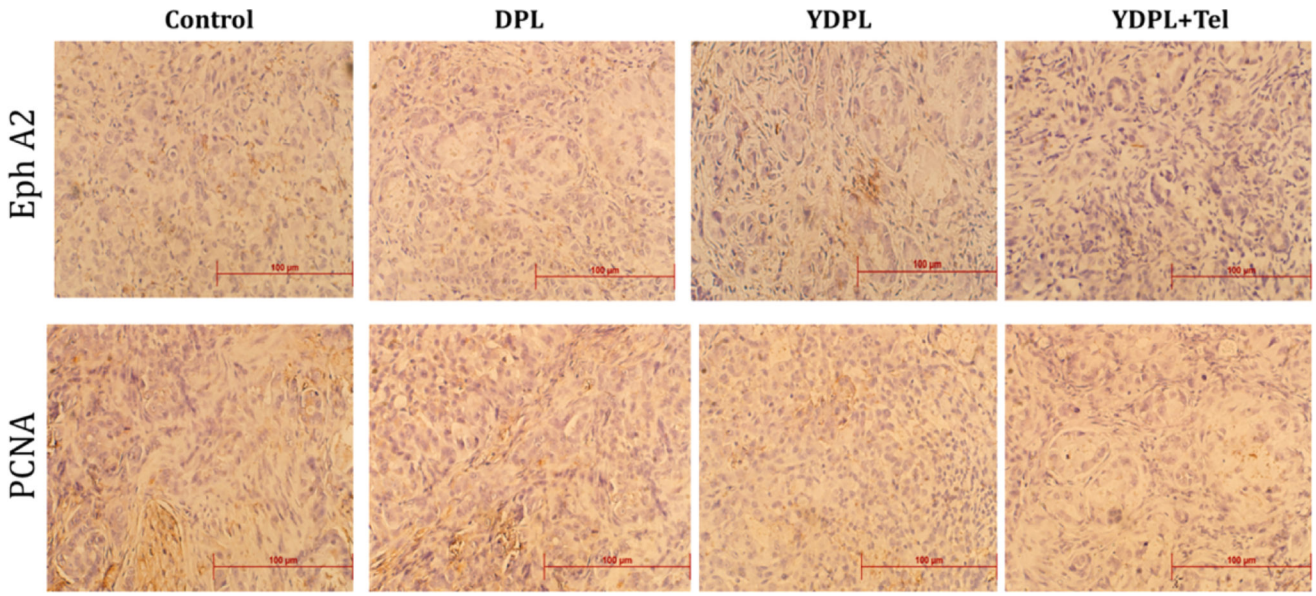

Figure 6.

Immunohistochemistry (IHC) analysis of lung tumor section for EphA2 and proliferation marker-PCNA. YDPL and YDPL + telmisartan treated groups showed marked reduction in expression of both markers.

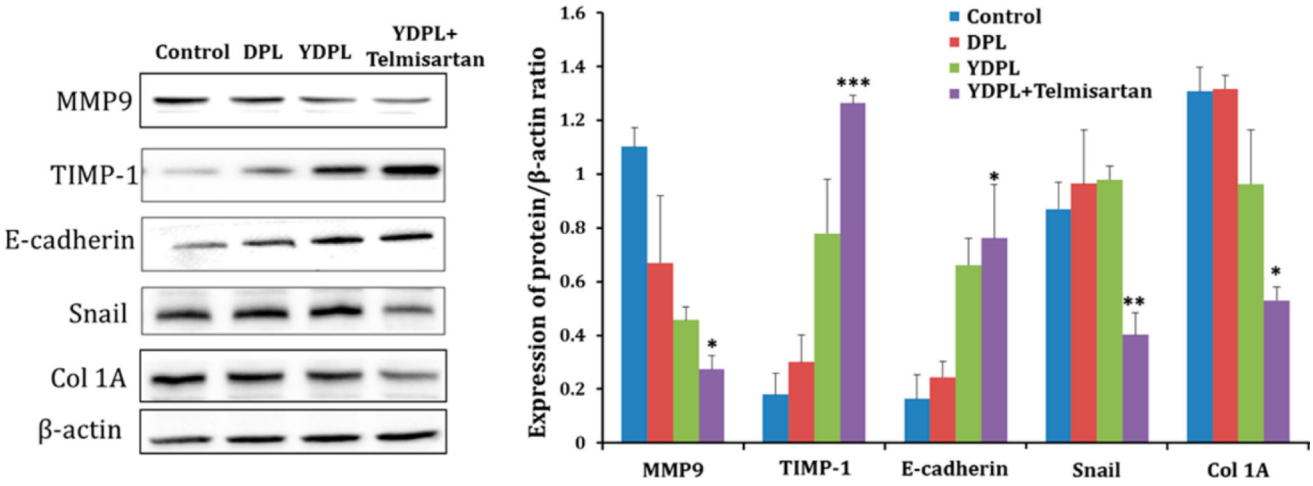

Figure 7.

Western blot analysis of lung tumor samples from various groups. Western blot images of different protein expressions in tumor lysates. Quantitative analysis of expressions of MMP9, TIMP-1, E-cadherin, snail, and col 1A. *$p < 0.05$ and **$p < 0.01$. Data were given as mean ± SD ($n = 3$).